Micromachined tunneling displacement transducers for physical sensors.

T.W. Kenny, W.J. Kaiser, J.A. Podosek, H.K. Rockstad,
J.K. Reynolds, and E.C. Vote.
Center for Space Microelectronics Technology
Jet Propulsion Laboratory
California Institute of Technology
Pasadena, CA 91109

Abstract

We have designed and constructed a series of tunneling sensors which take advantage of the extreme position sensitivity of electron tunneling. In these sensors, a tunneling displacement transducer, based on scanning tunneling microscopy principles, is used to detect the signal-induced motion of a sensor element. Through the use of high-resonant frequency mechanical elements for the transducer, sensors may be constructed which offer wide bandwidth, and are robust and easily operated. Silicon micromachining may be used to fabricate the transducer elements, allowing integration of sensor and control electronics. Examples of tunneling accelerometers and infrared detectors will be discussed. In each case, the use of the tunneling transducer allows miniaturization of the sensor as well as enhancement of the sensor performance.

Introduction

Devices used in the measurements of many physical quantities (position, motion, pressure, temperature, radiation) rely on measurement of a change in the relative separation between a pair of components. Changes in relative position are then detected through changes in the capacitance between the two elements,[1-3] through optical techniques,[4-6] or through flexing of piezoresistors.[7] In each case, large structures are often required to achieve sensitivities that are not limited by readout noise in the transducer. Recently, electron tunneling through a narrow vacuum barrier has been employed in Scanning Tunneling Microscopy (STM), to study the atomic scale structure of surfaces.[8] The tunneling current, I, has the following dependence on the separation, s, between a pair of metallic electrodes:

$$I \propto V \exp(- \alpha \sqrt{\Phi}\, s),$$

where Φ is the height of the tunneling barrier, V is the bias voltage, V is small compared to Φ, and $\alpha = 1.025$ ($Å^{-1}$ $eV^{-1/2}$).[8] For typical values of Φ and s, the current varies by an order of magnitude for each Å change in electrode separation. This sensitivity to relative position is superior to that available in other compact transducers and creates an opportunity for miniaturization of a broad class of sensors without loss of sensitivity. A position sensor based on electron tunneling has already been incorporated into the design for an accelerometer,[9,10] and a magnetometer.[11,12] Several other applications are being considered as well. Many of the fundamental issues, engineering issues and applications associated with tunneling sensors were recently discussed at the first Tunnel Sensors Workshop.[13]

Typical tunneling devices rely upon piezoelectric actuators. These actuators are known to suffer from sensitivity to thermal drifts, hysteresis, and creep in the response of the piezoelectric materials; these effects can impose limitations on the performance of existing tunneling devices. The development of miniature sensors which incorporate piezoelectrics is complicated by the variety of different materials required for the construction of the device.

There have been recent advances in the techniques for micromachining of silicon through the use of anisotropic etchants and doping to control etching.[14] These advances have led to the development

of a new class of sensors composed of micromachined silicon. The advantages to the development of sensor components in silicon include the use of single crystals as raw material, use of photolithography for precision patterning, and use of batch processing techniques to reduce fabrication costs. Micromachining has been used to construct miniature STMs.[15] More recently, surface micromachining techniques have been used to fabricate x-y scan stages for a tunneling accelerometer.[12,16] A surface micromachined structure in which tunneling has been demonstrated between adjacent elements has also been demonstrated. [17]

The micromachined tunneling displacement transducer can offer advantages in sensitivity, mass, and volume over conventional transducers. Other performance issues, such as stability and accuracy, will require experimental evaluation. Tunneling devices are well known to suffer from instability due to migration of atoms on the tunneling tip. These and other effects can result in low-frequency drifts in the output of the tunneling sensor.[18-22] Because the low-frequency drifts have not been well-characterized, we have chosen to focus on applications which are insensitive to low-frequency noise. In particular, accelerometers are needed for applications at frequencies above several Hz, and infrared detector applications require the use of choppers operating above several Hz. As sensors are built and tested, the use of tunneling for low-frequency measurements will be evaluated.

Accelerometer

We have designed and constructed a prototype electron tunneling accelerometer. In contrast to conventional tunneling devices, the relative position of the electrodes was controlled through use of electrostatic forces applied between the elements as shown in Fig. 1. In this case, the electrostatic forces induce deflection of a micromachined silicon cantilever spring. Use of the electrostatic actuator is important because of insensitivity to thermal drifts and immunity to creep. Various methods for manufacturing a suitable tunneling tip are available.[8,23] We have formed silicon tips directly from the substrate by undercutting a 60 μm x 60 μm square of SiO_2 with Ethylene Diamine Pyrocatechol (EDP). The active surfaces of all electrodes are prepared by evaporation of 3000 Å thick Au films through a shadow mask.

Once the device is assembled, a voltage is applied to the electrostatic deflection electrodes. This deflection voltage produces an attractive force between the electrodes, which deflects the spring. When the tip is within 10 Å of the counter electrode, a tunnel current is established. Active regulation of the tip-electrode separation using feedback control of the tunneling current is carried out as for STM.

For the Au electrodes in this device, measurements of Φ have given a value of 0.5 eV, which corresponds to a displacement responsivity of 0.94 nA/Å at an average current of 1.35 nA. This value of Φ is typical for our sensors and is consistent with STM measurements with gold electrodes. Given the measured noise, the sensitivity to variations in the tip-sample separation is 2×10^{-4} Å/$\sqrt{\text{Hz}}$ at a frequency of 1 kHz.[24] The responsivity of this sensor to changes in acceleration may be calculated. Below the resonant frequency of about 200 Hz, the responsivity is 3×10^{-5} A/g. With the observed noise of the sensor, the sensitivity is 1×10^{-7} g/$\sqrt{\text{Hz}}$ at 10 Hz. Since the measured noise includes contributions from accelerations in the laboratory, the actual sensitivity is probably better. This sensitivity is several orders of magnitude better than conventional miniature accelerometers.[1,12] Conventional accelerometers with comparable sensitivity are several orders of magnitude larger and heavier.

We are presently working on an improved accelerometer which features a lightweight, wide-bandwidth cantilever that is used to follow the motion of a suspended 50 mg proof mass. In this device, the feedback forces are applied to the cantilever instead of the proof mass. Since the feedback loop does not attempt to control the position of the proof mass, the loop may be operated both below and above the resonance of the proof mass. The bandwidth of the feedback loop is limited by the resonance of the cantilever, which is expected to exceed 10 kHz. With this modification, we expect to achieve acceleration sensitivity of 10^{-8} g/$\sqrt{\text{Hz}}$ over the entire band from 5 Hz to 1 kHz.

Infrared Sensor

An important application that is presently being investigated is the use of a tunnel transducer in a pneumatic infrared detector. Golay's original pneumatic detector consisted of a small cavity filled with gas at room temperature and separated from the surroundings by a window and

a thin membrane.[25-27] The membrane was coated on one side with a thin metallic film, which has significant absorption throughout the infrared whenever the sheet resistance of the film is approximately half of the impedance of free space.[28-30] The gas was heated by contact with the membrane, and expanded thermally, which forced the membrane to expand outward. This expansion is detected through optical or capacitive techniques.[31] These detectors are quite fragile, difficult to fabricate, and expensive. Nevertheless, they have been widely used, primarily because of their improvement in sensitivity over all other room-temperature detectors in the mid to far infrared.

With the above considerations in mind, we have begun the development of an improved pneumatic infrared detector. This detector is constructed of micromachined silicon, and uses a tunneling displacement transducer. An early prototype of this device consisted of a cavity of area $(0.1\ cm)^2$ and thickness 0.015 cm, filled with air at atmospheric pressure. This cavity is trapped between a pair of silicon wafers, one of which has been etched through to a 0.5 μm thick Si_xN_y membrane. These wafers are presently sealed using adhesive; silicon wafer bonding techniques are also available. The outer surface of the membrane is coated with ~100 Å of gold to serve as an electrode for tunneling as well as an efficient absorber of infrared radiation. A calculation of all the thermodynamic properties of the structure as well as the responsivity and contribution from various noise sources has been carried out.[32] This calculation is analogous to that performed for the original Golay cell. Noise sources that play an important role in this device include thermodynamic fluctuations in the temperature of the cell, shot noise in the transducer and fluctuations in background radiation. If we sum the theoretical contributions to the noise, and consider the 50% efficiency of the absorber, the predicted noise equivalent power (NEP) of the prototype is $6 \times 10^{-11}\ W/\sqrt{Hz}$ at low chopping frequencies. At frequencies below 10 kHz, the NEP is dominated by thermal fluctuations.

We have fabricated a prototype infrared sensor using the micromachined tunneling transducer described above.[23] The prototype infrared sensor was made operational, and infrared response was observed with a variety of laboratory blackbody sources. The measured NEP of this prototype is $8 \times 10^{-10}\ W/\sqrt{Hz}$ at 10 Hz. Noise in this prototype was

dominated by the sensitivity of the transducer to mechanical vibration. Nevertheless, the sensitivity of the tunneling infrared sensor is already competitive with the best commercial pyroelectric sensors. The sensitivity of this infrared sensor can be readily improved by as much as an order of magnitude through the use of an optimized transducer with less vibration sensitivity.

Improved Infrared Sensor

The original sensors based on the use of micromachined actuators with electrostatic deflection consisted of low-stiffness structures to allow their deflection over a considerable range (>100 μm).[23] These large deflections were necessary to achieve the 'coarse approach' as well as the 'fine control' with a single technique. Prototype transducers based on this design were operated and characterized. These prototype devices were based on simple micromachining techniques, and consisted of folded cantilever springs with a total mass of about 30 mg, and a total area of about 2 cm^2. Displacement sensitivities of 0.001 $Å/\sqrt{Hz}$ were measured with these prototype tunneling transducers.

The requirement for deflection over a considerable range with electrostatic forces led to resonant frequencies of the moving transducer element of less than 200 Hz. To achieve stability in the control of these elements, the bandwidth of the feedback control system was restricted to less than this resonant frequency. Unfortunately, the bandwidths required for many important measurement applications may be as large as 10 kHz.

In addition, it is important for any transducer to be insensitive to environmental sources of noise. For example, an infrared detector should be insensitive to vibration. Since the tunneling transducer is fundamentally a mechanical structure, the sensitivity to vibration is to be eliminated through careful mechanical design. When a sensor element is subjected to an acceleration at signal frequencies below its mechanical resonance, the amplitude of deflection is inversely proportional to the square of the resonant frequency. Therefore, sensitivity to vibration is best reduced by increasing the resonant frequency of the elements of the transducer.

To meet the operational requirements for sensing applications of a tunneling transducer, we have designed a new series of micromachined

actuators. These new actuators are important because they are designed to offer resonant frequencies above 10 kHz. The new actuators achieve the higher resonant frequencies primarily through reduction in actuator mass by more than 4 orders of magnitude. As a result, the new actuators have smaller range of deflection (<5 μm), which precludes their use for coarse approach between tunneling electrodes. Through the use of micromachining techniques, it is possible to assemble sensors with the electrode spacing well within the range of the actuator, thereby accomplishing the coarse approach during assembly.

The primary wide-bandwidth actuator consists of a diaphragm. These diaphragms are fabricated by coating the front surface of a silicon wafer with low-stress LPCVD silicon nitride. The diaphragms are released by etching square holes through the wafer from its back surface with a chemical etchant that does not etch silicon nitride, such as EDP. A drawing of a diaphragm positioned above the tunneling and deflection electrodes is shown in Fig. 2. This actuator was designed for an infrared detector that will be used to detect variations in infrared power. For the infrared sensor, the dimensions of the membrane are 2 x 2 mm^2 x 0.5 μm. The resonant frequency and stiffness for an unstressed diaphragm of these dimensions are calculated to be 20 kHz and 2 N/m respectively. The linear range of deflection for this actuator may be extended by corrugating the diaphragm. We have fabricated corrugated diaphragms by etching concentric circular depressions with depth of 1μm and pitch of 10 μm into a silicon substrate before deposition of the low-stress nitride. The fabrication and characterization of the infrared sensor will be described elsewhere.[33]

The device is assembled by bonding the substrate in a 28-pin test socket with epoxy, connecting the electrodes to the pins by gold wire-bond, and inserting the test package in a circuit board. The membrane element is placed on the substrate and oriented properly. A mechanical clamp holds the elements together while voltages are applied. Some minor adjustment of membrane position is typically required to allow tunneling. Then, more epoxy is applied to bond the membrane within the package, and the clamps are removed. Using this procedure, a set of nominally identical sensors can be made operational at deflection voltages which

vary by 10-20%. This variation is attributed to variations in clamping force during assembly, as well as to wafer surface roughness.

This device is operated in the following manner. A 150 mV tunneling bias is applied to the tip, and the electrode on the membrane is grounded. A large voltage (100-200V) is applied to the deflection electrodes, electrostatically attracting the membrane down towards the tip. When the membrane is within 10 Å of the tip, a tunnel current of 1 nA appears. The feedback loop compares this current to a reference value, and applies an error signal to the deflection electrode, thereby maintaining the position of the actuator. If a force is applied to the actuator, the feedback loop responds with a balancing force that keeps its position fixed.

Conventional STM feedback loops are complicated by the presence of a low-frequency actuator resonance appearing near the feedback loop operating band. With the lowest mechanical resonant frequency of these actuators being above 10 kHz, the gain and bandwidth of the electrical circuit used to control the sensor may be substantially larger than that used in typical STMs or in previous tunneling sensors. Because of this, the feedback circuitry used may be simplified. Figure 3 shows a typical feedback circuit that has been used to control tunneling between a micromachined tip and the diaphragm actuator.

A voltage drop across a 10 MΩ resistor in series with the tip occurs with tunneling. A low-noise operational amplifier (CA3140) in follower configuration is positioned near the transducer to lower the source impedance and allow direct measurement of the voltage. A simple op-amp circuit (CA3140) is then used to compare the preamplifier output with a set-point and generate an error signal. This low-voltage, wide-bandwidth error signal is then added to a high-voltage, narrow-bandwidth offset to produce the voltage that is applied to the deflection electrodes. The high voltage signal may be generated by a power supply that is initially adjusted to set the error signal near zero.

If the error amplifier is located near the transducer, the preamplifier may be eliminated. The resulting feedback circuit requires only a single operational amplifier, an external offset voltage, and a few fixed-value resistors.

These transducers were made operational and routine characterizations were carried out. Stable tunneling was achieved in one

typical transducer with an average deflection voltage of 120 V. Figure 4 shows a measurement of the voltage noise from the feedback circuit measured at the error amplifier, and at the deflection electrode. The signal at the deflection electrode is smaller because of the low-pass filter which consists of the resistor network and the stray capacitance at the deflection electrode. The 120 V deflection voltage exerts a total force of 2 x 10^{-5} N on the central 0.7 mm^2 area of the membrane, causing a measured deflection of about 1 μm. The displacement responsivity of this actuator is given by:

$$\frac{\partial s}{\partial V} = \frac{\partial s}{\partial F}\frac{\partial F}{\partial V} = \frac{1\ \mu m}{2 \times 10^{-5}\ N}\ \frac{2\varepsilon A\, V}{s^2}$$

$$= (0.5\ m/N)\ (3.3 \times 10\text{-}7\ N/V) = 1.7 \times 10^{-8}\ m/V$$

With the measured voltage noise of the transducer operating in air in the laboratory as shown in Fig. 4, the displacement sensitivity may be calculated. The measured displacement sensitivity of this transducer is then 0.017 $Å/\sqrt{Hz}$ at 10 Hz and 0.0002$Å/\sqrt{Hz}$ at 10 kHz.

A 10 Hz oscillation voltage was added to the reference input of the feedback loop, causing a 0.1 nA oscillation in the tunneling current. To produce this oscillation, the feedback loop adds a small voltage oscillation to the deflection voltage, which was measured to be 2.5 mV in amplitude. From Eq. 1, the height of the tunnel barrier, ϕ, is given by :

$$\sqrt{\phi} = \frac{1}{I}\frac{\partial I}{\partial s} = \frac{1}{I}\ \frac{\partial I}{\partial V}\ \frac{\partial V}{\partial s} = \frac{1}{1.22\ nA}\ \frac{0.1\ nA}{0.0025\ V}\ \frac{1}{170\ Å/V}$$

ϕ = 0.41 V.

At different times and with different sensors, this barrier height may vary by as much as a factor of 2. Since the feedback loop applies rebalance forces to maintain the position of the membrane, any variation in barrier height will produce a variation in the transducer noise. The transducer responsivity will not be affected by variations in ϕ.

Figure 5 shows a measurement of the bandwidth of the transducer. For this measurement, a white noise voltage modulation is added to the reference input of the error amplifier in the feedback loop. The feedback loop responds by generating an amplified modulation signal at the deflection electrode, which produces modulations in the position of the

membrane, as well as modulations in the tunneling current. Figure 5 shows the ratio of the measured modulations in tunnel current to the white-noise modulation as a function of frequency, recorded by a standard spectrum analyzer. At all frequencies up to 50 kHz, the transducer is able to accurately reproduce the white noise modulations. Above 50 kHz, this response begins to roll off because of the limited bandwidth of the preamplifier. Figure 6 shows the phase shift between the measured modulations and the white noise modulations. This phase shift is less than 5 degrees for frequencies below 10 kHz, increasing to 30 degrees at 50 kHz. At frequencies above 100 kHz, capacitive coupling between the noise source and the transducer contributes to the measurement, as evidenced by the variation in the phase shift at those frequencies.

This transducer is presently being used as part of the electron tunneling infrared sensor.

Summary

We have constructed a series of tunneling displacement transducers. The most recent devices, which are based on high-resonant frequency mechanical elements can be used for measurements of physical signals at frequencies as high as 50 kHz. Sensors based on the use of tunneling transducers with wide control bandwidths are presently being designed, built and tested.

The work described in this paper was performed by the Center for Space Microelectronics Technology, Jet Propulsion Laboratory, California Institute of Technology and was jointly sponsored by the Strategic Defense Initiative Organization/Innovative Science and Technology Office, the Defense Advanced Research Projects Agency, the Naval Air Development Center, the Army Space Technology Research Office, The Office of Naval Technology, and the National Aeronautics and Space Administration, Office of Aeronautics, Exploration, and Technology.

References

[1] F. Rudolf, Sensors and Actuators 4, 191 (1983).

[2] K.E. Petersen, A. Shartel and N. Raley, IEEE Trans. Electron Devices ED-29, 23 (1982).

[3] C.S. Sander, J.W. Knutti, and J.D. Meindl, IEEE Trans. Electron Devices ED-27, 927 (1980).

[4] E. Stemme and G. Stemme, IEEE Trans. Elect. Dev. 37, 648 (1990).

[5] D.L. Gardner, T. Hofler, S.R. Baker, R.K. Yarber and S.L. Garrett, J. Lightwave Tech. LT-5, 953 (1987).

[6] D. Rugar, Rev. Sci. Instrum. 59, 11 (1988).

[7] H.V. Allen, S.C Terry and D.W. De Bruin, Sensors and Actuators 20, 153 (1989).

[8] G. Binnig and H. Rohrer, IBM J. Res. Develop. 30, 355 (1986).

[9] S.B. Waltman, W.J. Kaiser, Sensors and Actuators 19, 201 (1989).

[10] A.A. Baski, T.R. Albrecht and C.F. Quate, J. of Microscopy 152, 73 (1988).

[11] J.H. Wandass, J.S. Murday, and R.J. Colton, Sensors and Actuators 19, 211 (1989).

[12] R.A. Brizzolara, RJ. Colton, M. Wun-Fogle, and H.T. Savage, Sensors and Actuators 20, 199 (1989).

[13] Proceedings of the 1992 Tunnel Sensors Workshop, Jet Propulsion Laboratory, Pasadena, CA, to be published (1992).

[14] K.E. Petersen, Proc. IEEE 70, 420 (1982).

[15] S. Akamine, T.R. Albrecht, M.J. Zdeblick, and C.F. Quate, IEEE Electron Device Lett. 10, 490 (1989).

[16] J.J. Yao, S.C. Arney, and N.C. MacDonald, J. Microelectromechanical Sys. 1,14 (1992).

[17] D. Kobayashi, T. Hirano, T. Furuhata, and H. Fujita, Proceedings of 1992 Tunnel Sensors Workshop, to be published (1992).

[18] M.E. Welland and R.H. Koch. Appl. Phys. Lett. 48, 724 (1986).

[19] J.B. Pendry, P.D. Kirkman and E. Castano, Phys. Rev. Lett. 57, 2983 (1986).

[20] M.F. Bocko, K.A. Stephensen, and R.H. Koch, Phys. Rev. Lett. 61, 726 (1988).

[21] B. Yurke and G.P. Kochanski, Phys. Rev. B 41, 8184 (1990).

[22] D.W. Abraham, C.C. Williams, and H.K. Wickramasinghe, Appl. Phys. Lett. 53, 1503 (1988).

[23] R.B. Marcus, T.S. Ravi, T. Gmitter, K. Chin, D. Liu, W.J. Orvis, D.R. Ciarlo, C.E. Hunt and J. Trujillo,. Appl. Phys. Lett. 56, 236 (1990).

[24] T.W. Kenny, S.B. Waltman, J.K. Reynolds, and W.J. Kaiser, Appl. Phys. Lett. 58, 100 (1991).

[25] M.J.E. Golay, Rev. Sci. Inst. 18, 347 (1947).

[26] M.J.E. Golay, Rev. Sci. Inst. 20, 816 (1949).

[27] A. Hadni, Essentials of Modern Physics Applied to the Study of the Infrared (Pergamon, Oxford, 1967) pp 269-283.

[28] L.N. Hadley, D.M. Dennison, J. Opt. Sci. Am. 37, 451 (1947).

[29] C. Hilsum, J. Opt. Sci. Am. 44, 188 (1954).

[30] A. Hadni, ibid. pp. 252-7.

[31] M.J.S. Smith, L. Bowman, J.D. Meindel, IEEE Trans. Biomed. Eng. BME-33, 163 (1986).

[32] T.W. Kenny, W.J. Kaiser, S.B. Waltman, and J. K. Reynolds, Appl. Phys. Lett. 59,1820 (1991).

[33] T.W. Kenny, W.J. Kaiser, J.A. Podosek, H.K. Rockstad, and E.C. Vote, to be published

Figures and Captions

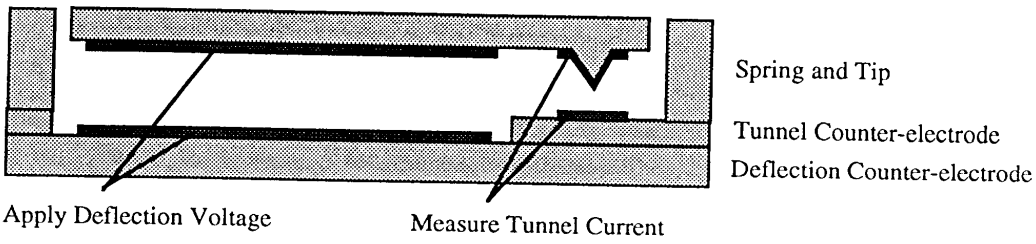

Figure 1 Conceptual drawing of prototype tunneling accelerometer. The upper plate is suspended by a micromachined spring and is deflected downward by electrostatic force. When the tip is within 10 Å of the tunnel counter-electrode, tunneling current is detected by the feedback loop. The feedback loop controls the deflection voltage so as to keep the upper plate in the same relative position. During acceleration of the sensor, the feedback force balances the inertial force. The deflection voltages are recorded as signal.

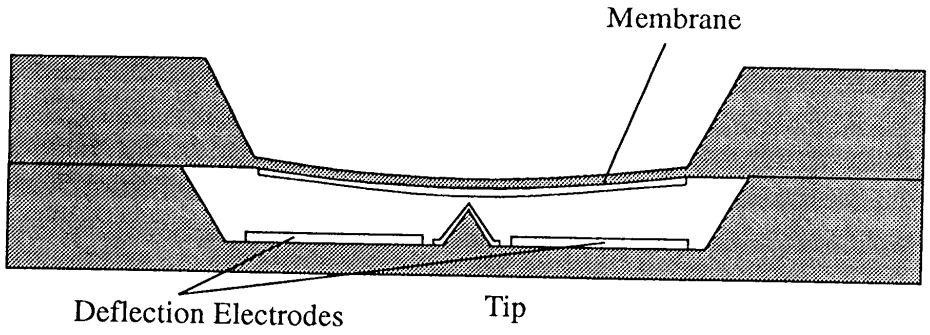

Fig. 2 Drawing of the membrane actuator. Electrostatic forces are used to deflect a thin membrane to within 10 Å of a fixed tunneling tip. The feedback circuit measures the tunnel current and applies correction voltages to the deflection electrodes so as to keep the membrane position fixed. Any physical forces applied to the membrane are balanced by the feedback circuit.

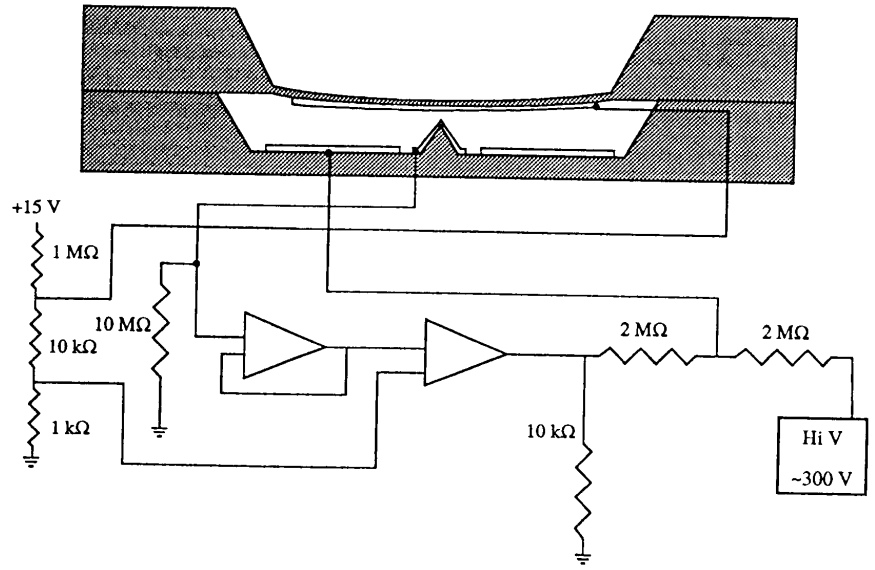

Fig. 3 This drawing shows the feedback circuit that is used to control the tunneling transducer. A bias of 150 mV is applied to a 10 MΩ resistor in series with the tunneling tip. The appearance of a tunneling current results in a voltage drop at the input of the optional preamplifier, which is operated in follower configuration. A second amplifier compares the measured voltage with a reference value and produces an error signal. The error signal is added to a high-voltage offset and applied to the deflection electrode.

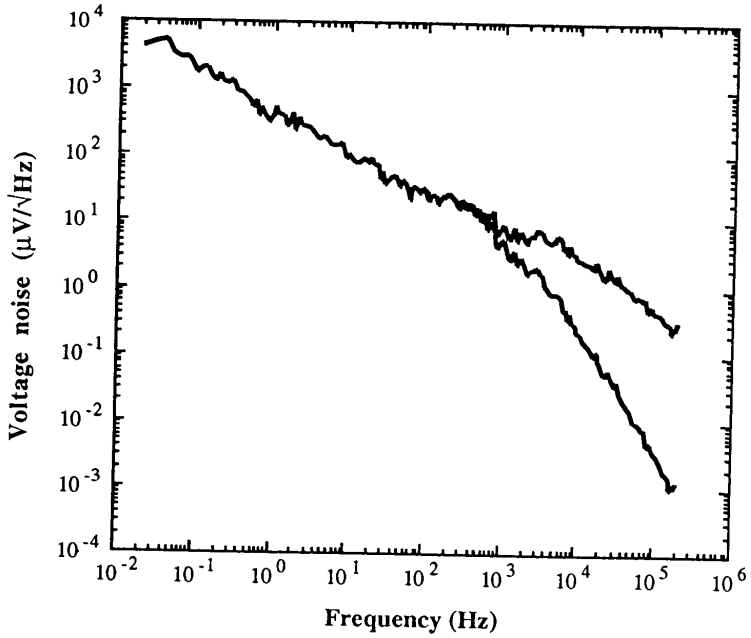

Fig. 4 This plot shows the measured voltage noise at the output of the feedback loop during operation of a tunneling transducer. The upper curve is recorded at the output of the error amplifier, while the lower curve is recorded at the deflection electrode.

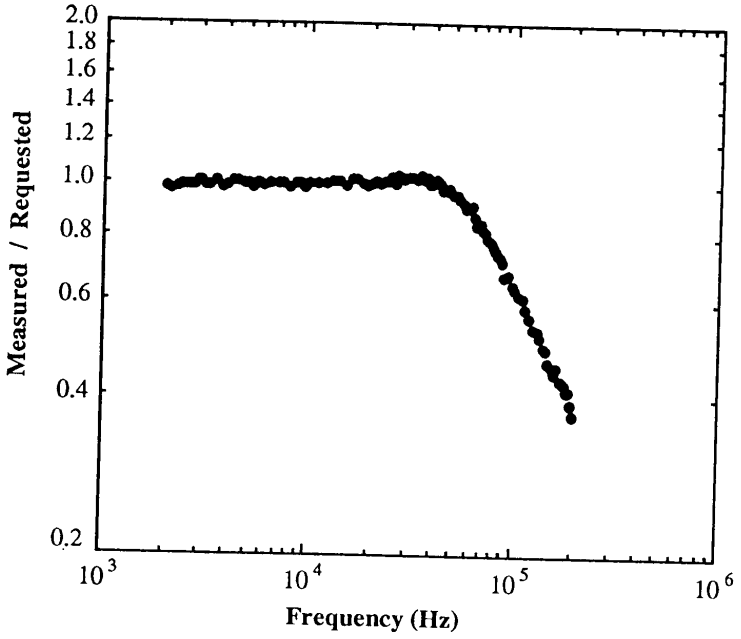

Fig. 5 This plot shows the ratio of measured modulation to input white noise modulation in the tunneling current as a function of frequency for frequencies between 2 kHz and 200 kHz. The feedback control system is able to reproduce the white noise modulation at all frequencies up to 50 kHz.

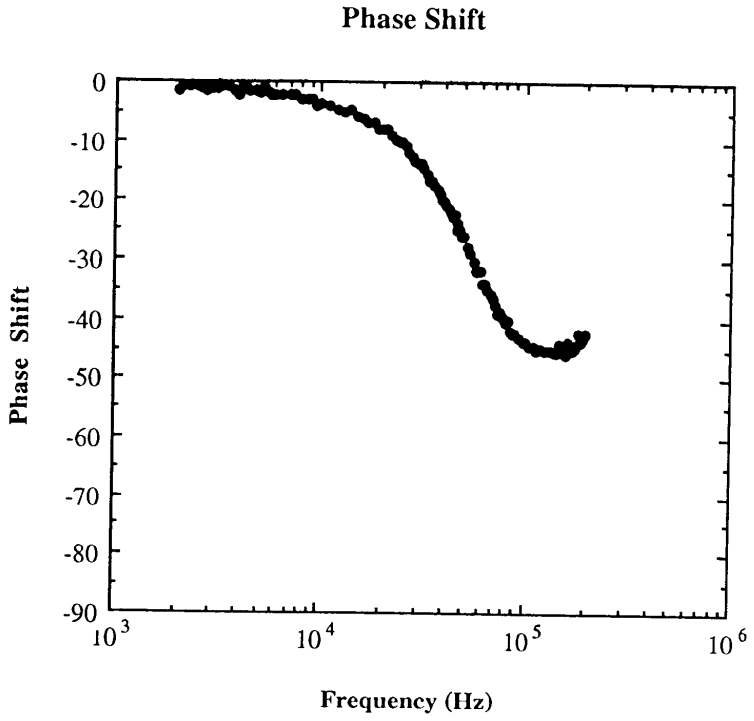

Fig. 6 This plot shows the phase shift between the measured and requested oscillation in tunneling current for frequencies between 2 kHz and 200 kHz. The phase shift is less than 5 degrees for frequencies below 10 kHz, but increases to 30 degrees at 50 kHz. Coupling between the noise generator and the transducer leads to errors in this measurement above 100 kHz.